



Effect of surface dissolution on kinetic parameters in flotation of ilmenite from different gangue minerals

Omid SALMANI NURI¹, Mehdi IRANNAJAD¹, Akbar MEHDILO^{1,2}

1. Department of Mining and Metallurgical Engineering, Amirkabir University of Technology, Tehran, Iran;

2. Department of Engineering, University of Mohaghegh Ardabili, Ardabili, Iran

Received 9 December 2018; accepted 20 October 2019

Abstract: The effects of acid surface dissolution on the flotation kinetics of ilmenite (IL) and its common accompanied gangue minerals including olivine-pyroxene (Ol-Px), tremolite-clinocllore (Tr-Cch) and quartz were investigated. The results show that through the surface dissolution the adsorption rate constant for ilmenite increases from 5.272 to 8.441 mol/(g·min) while it decreases for Ol-Px, Tr-Cch and quartz from 6.332, 7.309 and 7.774 mol/(g·min) to 5.034, 6.223 and 7.371 mol/(g·min), respectively. Also, the flotation experiments on a binary mixture of minerals indicate that after surface dissolution the values of modified rate constant for ilmenite flotation from Ol-Px, Tr-Cch and quartz are enhanced from 36.15, 36.52 and 47.86 min⁻¹ to 41.72, 45.78 and 56.24 min⁻¹, respectively. This results in the improvement of kinetic selectivity index (SI) in the separation of treated ilmenite from gangue minerals. As evidenced by ICP-MS analysis, the decrease of kinetic parameters for gangue minerals can be due to the removal of Fe²⁺, Ca²⁺ and Mg²⁺ ions from their surfaces, which results in the lack of enough active sites to interact with collector species. As confirmed by contact angle measurements, this prevents the formation of a stable hydrophobic layer on the minerals surfaces for creating stable attachments between minerals and bubbles. Generally, the improvement of ilmenite flotation kinetics has a negative correlation with the iron content in its accompanied gangue minerals.

Key words: surface dissolution; flotation; kinetic parameters; modified rate constant; selectivity index; collector adsorption

1 Introduction

Flotation is an extensively used separation method in the mineral beneficiation processes which has been found based on the differences between the surface properties of valuable and gangue minerals. These differences are commonly caused by flotation reagents including collector, depressant and activator [1–5]. In addition of flotation agents, some surface modification methods such as microwave radiation, preheating technique and surface dissolution have been recently used for creating suitable differences on the surface properties of minerals, and improving the floatability of valuable minerals [6–10]. In this regard, ilmenite has been widely considered due to its poor floatability. In ilmenite flotation, the Ti⁴⁺ ions and titanate species are active sites in acidic pH ranges while the Fe²⁺ ion and its hydroxyls are the active species at the weak acidic and alkaline pHs for reacting with a collector. Thus, in each mentioned pH range, only half of the surface ions are

active to react with the collector species. This leads to the poor floatability of ilmenite in comparison with rutile and magnetite minerals [11,12]. The acid surface dissolution pretreatment is one of the above mentioned methods which have been successfully utilized for modification of ilmenite surface properties and improvement of its flotation behavior [5,13,14]. The improvement of ilmenite floatability has been attributed to the conversion of Fe²⁺ ions to Fe³⁺ ones, which results in the formation of more stable ferric iron oleate in comparison with ferrous iron oleate on the surface of this mineral [13,14].

However, the effect of surface dissolution on the surface properties of ilmenite has been investigated in the previous works but the influence of this pretreatment method on the flotation kinetics significantly has not ever been considered. Thus, the present study is undertaken to investigate the effect of acid surface dissolution on the kinetics of collector adsorption and the flotation kinetics of ilmenite and its usual associated gangue minerals such as olivine, pyroxene, tremolite,

clinochlore, and quartz. This was performed by carrying out the flotation experiments for floating ilmenite from binary mixtures of ilmenite and gangue minerals and applying various kinetic models before and after surface dissolution. Also, some analytical methods such as inductively coupled plasma mass spectroscopy (ICP-MS), UV-visible analysis and contact angle measurements were used for studying the surface properties of minerals before and after pretreatment.

2 Kinetic models in adsorption and flotation

Adsorption kinetics is an important factor which affects the capacity of adsorption by changing the contact time [15]. The pseudo-first and second order models were used for modeling the kinetic rates of collector adsorption on the minerals surfaces [16,17]. These models are expressed as follows:

$$\lg(S_e - S_t) = \lg S_e - \frac{k_1}{2.303} t \quad (1)$$

$$\frac{t}{S_t} = \frac{1}{k_2 S_e^2} + \frac{1}{S_e} t \quad (2)$$

where S_t refers to the amount of collector uptake capacity at a particular time t ; S_e is the uptake at equilibrium time; k_1 and k_2 are the rate constants for the pseudo-first-order and second-order models, respectively.

The essential aim of the flotation kinetics is considering and deducing the changes in ultimate recovery (R_∞) and flotation rate constant (k). These factors are significant and can often be confusing [18]. Different kinetic models can be applied to analyzing the batch flotation results. It has already been shown that the flotation process follows the first-order kinetics [19–22]. Batch flotation test data in the literatures [23–26] support the first-order rate which can be reasonably used to determine the kinetic parameters. In this study, four different kinetic models, including classical model, Klimpel model (model with the rectangular distribution of floatability), modified Kelsall model (model with fast and slow-floating components), and fully mixed model have been used to evaluate the batch flotation results. These models are summarized in Table 1. The kinetic parameters (R_∞ and k) have been determined by model

Table 1 Models applied and implemented in Mathematica software

Model	Equation	
Model 1: Classical model	$R=R_\infty(1-e^{-kt})$	(3)
Model 2: Klimpel model	$R=R_\infty[1-(1/kt) \times (1-e^{-kt})]$	(4)
Model 3: Modified Kelsall model	$R=R_\infty[(1-z)(1-e^{-k_f t}) + z(1-e^{-k_s t})]$	(5)
Model 4: Fully mixed reactor model	$R=R_\infty\{1-[1/(1+t/k)]\}$	(6)

fitting to the experimental data using mathematical software [27].

In Table 1, R is the recovery of components at the time t ; z denotes a fraction of flotation component with the slow rate constant; k_s is a rate constant for slow floating component; k_f is a rate constant for fast floating component.

3 Experimental

3.1 Materials

The purified samples of ilmenite (IL), olivine-pyroxene (Ol-Px), tremolite-clinochlore (Tr-Cch) and quartz (Q) were used to perform the experiments of flotation kinetics. The handpicked samples obtained from the Qara-Aghaj titanium deposit were ground to 100% less than 150 μm using laboratory crushing and milling stages. 150 μm is a size which has been determined as liberation degree of ilmenite [28]. The different stages of wet sieving, tabling, and low and high-intensity magnetic separation methods were used to prepare the purified samples. Due to the similarities of surface properties of olivine and pyroxene minerals with each other as well as the surface properties of tremolite and clinochlore, the binary mixture of these minerals was separated from each other [29]. Table 2 lists the chemical composition of purified samples which are determined using XRF. Sodium oleate and pine oil were consumed as the collector and frother agents, respectively. Sodium hydroxide and sulfuric acid were used as pH regulator reagents through the flotation tests. The oxalic acid was used as a surface dissolution medium. In some tests, it was also applied as a pH regulator agent.

Table 2 Chemical composition of purified samples (wt.%)

Sample	TiO ₂	Fe ₂ O ₃	MnO	V ₂ O ₅	P ₂ O ₅	CaO	MgO	SiO ₂	Al ₂ O ₃	L.O.I
Ilmenite (IL)	46.2	48.6	1.04	0.29	0.24	0.38	2.53	0.19	0.44	0.0
Olivine-pyroxene (Ol-Px)	0.86	42.7	0.64	0.015	3.32	5.1	15.9	29.6	1.08	0.0
Tremolite-clinochlore (Tr-Cch)	0.74	17.7	0.17	0.056	0.075	5.96	19.7	43.1	4.9	7.1
Quartz (Q)	—	0.28	—	—	—	0.35	—	98.1	0.66	0.36

3.2 Methods

3.2.1 Batch flotation

The batch flotation tests were conducted on the purified samples using a Denver DR-12 flotation machine in a one-liter cell. In all flotation experiments conducted at a constant pH of (6.3±0.02) as an optimal pH determined in the previous works [30–33], the impeller speed and solid mass fraction were fixed at 1400 r/min and 30%, respectively. After mixing the pulp for 5 min, 1000 g/t of sodium oleate as a collector was added to the cell and conditioned for 5 min. After then 100 g/t of pine oil with 2 min of conditioning time was added to the pulp, and the air was opened and flowed inside the cell. Finally, the froth phase was collected at interval time of 0.5, 1, 1.5, 3, 5, 8, 12, and 15 min. The froth phase was scraped every 10 s. The taken samples of concentrate and tailing were filtered, dried, and assayed. In the flotation experiments on a binary mixture of IL+OI-Px, IL+Tr-Cch, and IL+Q before and after surface dissolution for studying the particle flotation rate and ultimate recovery, the mass ratio of ilmenite to gangue minerals was considered 20 wt.% to 80 wt.%.

3.2.2 Surface dissolution

The surface dissolution of the purified samples prior to the flotation tests was carried out by mechanical stirring in a 7.5 vol.% oxalic acid solution at a pH of 1 for 10 min. After then, the liquid phase was filtered, and the solid phase was washed for 5 min with double distilled water and was dried at room temperature.

3.2.3 Contact angle

Sessile drop method was used for contact angle measuring of the minerals before and after surface dissolution. A drop of distilled water was put on the polished section of mineral which is prepared at the desired condition. After then, an image was taken by a camera, and the contact angle was measured using Image J software.

3.2.4 ICP-mass analysis

The ICP-mass analysis was used to investigate the amount of transferred elements from the mineral surfaces into the acid solution [13]. The CETAC ADX-500 auto-diluter system was tested with ELAN® v 2.1 software and the ELAN 6000 ICP-MS instrument to determine on-line automated dilution performance during the analysis of standard solutions. In order to prepare the samples to ICP analysis, 5 g of purified samples were placed in a beaker which was then filled with the oxalic acid solution. The suspension was agitated with a mechanical stirrer for 15 min. After filtration of the suspension, the remaining liquid phase was analyzed by ICP-MS.

3.2.5 UV-visible analysis

The adsorption amount of collector on the surface of minerals was measured using UV-visible spectro-

photometer (UV-1601, Beijing Beifen-Ruili Analytical Instrument Co., Ltd.) at $\lambda=192$ nm [34]. In each test, 1 g of purified mineral sample with a size of 45 to 150 μm was added to the 50 mL of double deionized water. The solution was equilibrated at the flotation condition and then filtered. The equilibrium for the present study was attained at 100 min.

3.2.6 Calculations

The recovery of minerals in the flotation concentrate was calculated by Eq. (7), which is known as Wills and Napier-Munn equation:

$$R = \frac{Cc}{(C+T)f} \times 100\% \quad (7)$$

where R is the recovery of ilmenite (%); C and T are the dry masses of concentrate and tailing, respectively; c and f are the ilmenite contents (wt.%) in the concentrate and feed, respectively.

The adsorption of the collector was calculated by

$$q_t = \frac{(C_0 - C_t)V}{m} \quad (8)$$

where C_0 and C_t refer to the initial and final concentrations of sodium oleate in the solution (mol/L), respectively; V is the volume of solution (L); m is the mass of the mineral sample (g); q_t is the adsorption density of collector (mol/g).

4 Results and discussion

4.1 Flotation experiments

4.1.1 Flotation of ilmenite from binary mixtures

Figure 1 shows the recovery of ilmenite flotation from the binary mixtures of different gangue minerals as a function of flotation time before and after pretreatment. For both states, two regions are observed in the recovery-time curves. Before surface dissolution (Fig. 1(a)), the first region shows that the flotation recovery occurs quickly in the first 3 min, and the second region represents the increase of recovery in the plateau region. After 15 min, the flotation recovery of untreated ilmenite varies from 72.2% to 80.6% in the presence of different gangue minerals. As shown in Fig. 1(b), after surface dissolution, the occurrence of fast-rising of flotation recovery in the first region takes about 5 min. The second region is similar to that of untreated one, but the flotation recovery of treated ilmenite is higher, and changes from 76.4% to 90.8%. This means that the surface dissolution increases the ultimate recovery of ilmenite flotation significantly. Also, the results show that the time of fast flotation stage (first region) enhances from 3 to 5 min after surface dissolution. This means that the rate constant of ilmenite flotation is increased after pretreatment.

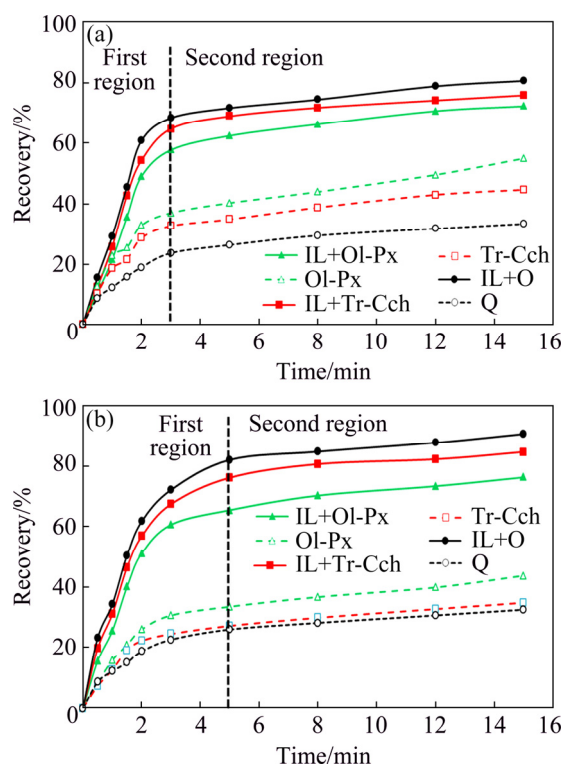


Fig. 1 Accumulated recovery of minerals versus flotation time before (a) and after (b) surface dissolution (pH: 6.3; solid fraction: 30%; collector dosage: 1000 g/t; pine oil dosage: 100 g/t)

The flotation recoveries of ilmenite from different binary mixtures of gangue minerals are as follows: $IL+Q > IL+Tr-Cch > IL+Ol-Px$.

On the other hand, the results show that the orders of gangue recoveries in the ilmenite concentrate are as follows: $Ol-Px > Tr-Cch > Q$.

The flotation recovery of gangue minerals has a positive correlation with their iron content. Thus, the selective flotation of ilmenite from Ol-Px containing a higher amount of Fe is more difficult than Tr-Cch and quartz phases. As shown in Fig. 1(b), the differences between ilmenite recovery and all the gangue minerals are increased after surface dissolution. This means that the surface dissolution not only increases the ilmenite floatability but also decreases the recovery of gangue minerals. The results are in good agreement with the previous works [13,14].

4.1.2 Flotation kinetic models

Figures 2(a–f) present the fitting of kinetic models for the cumulative recovery as a function of flotation time before and after surface dissolution. The results display that the classical model and Klimpel model have the best and the weakest fits for experimental recoveries, respectively. Also, the modified Kelsall model has a good fit to the experimental data.

The classical model with the best fit to the experimental data is used to determine and compare the

kinetic parameters before and after surface dissolution. The results of estimated kinetic parameters by the classical model for binary mixtures of minerals are presented in Table 3. The results show that both k and R_{∞} are increased for the pretreated ilmenite in the presence of all gangue minerals. These kinetic parameters are decreased for the pretreated Ol-Px and Tr-Cch minerals, while they have not significant changes for the pretreated quartz. Also, the accuracy of the classical model for all minerals is well proved by the value of $R^2 > 0.99$.

4.1.3 Modified rate constant (K_m) and kinetic selectivity index (SI)

In many laboratory tests, the comparison of flotation kinetics data is difficult. Because the change in condition results in some changes in both ultimate recovery and rate constant. In this regard, the modified rate constant and the kinetic selectivity index (SI, I_s) defined according to Eqs. (9) and (10) [19,35–38] can be used to compare the results.

$$K_m = k \cdot R_{\infty} \quad (9)$$

$$I_s = K_{m_1} / K_{m_2} \quad (10)$$

where K_{m_1} and K_{m_2} are the modified rate constants of ilmenite and gangue minerals, respectively.

The results of the comparison between K_m and I_s values for the flotation of ilmenite from studied gangue minerals are shown in Figs. 3 and 4 before and after surface dissolution. Figure 3 indicates that after surface dissolution the K_m values for ilmenite flotation in the presence of Ol-Px, Tr-Cch, and quartz are increased from 36.15, 36.52 and 47.86 min^{-1} to 41.72, 45.78 and 56.24 min^{-1} , respectively. In the case of gangue minerals, while after surface dissolution the K_m value for quartz keeps approximately constant, and it is significantly decreased for Ol-Px and Tr-Cch samples. As observed in Fig. 4, before pretreatment, the kinetic selectivity index for ilmenite flotation from quartz as an iron lacking mineral is greater than that of Ol-Px and Tr-Cch samples. The higher selectivity index represents a better separation of valuable minerals from gangues. Thus, the separation of ilmenite from quartz using flotation process can be done more selectively than that from two other gangue phases. After surface dissolution, the kinetic selectivity index is increased for the treated ilmenite in the presence of various gangue minerals. This increase for treated Tr-Cch mineral phase is higher than that of treated Ol-Px and quartz minerals. In other words, the kinetic selectivity index for the flotation of treated ilmenite from treated Tr-Cch is very close to that of untreated quartz. Generally, these results show that the surface dissolution improves the selectivity of ilmenite separation from gangue minerals, especially from low iron content gangues.

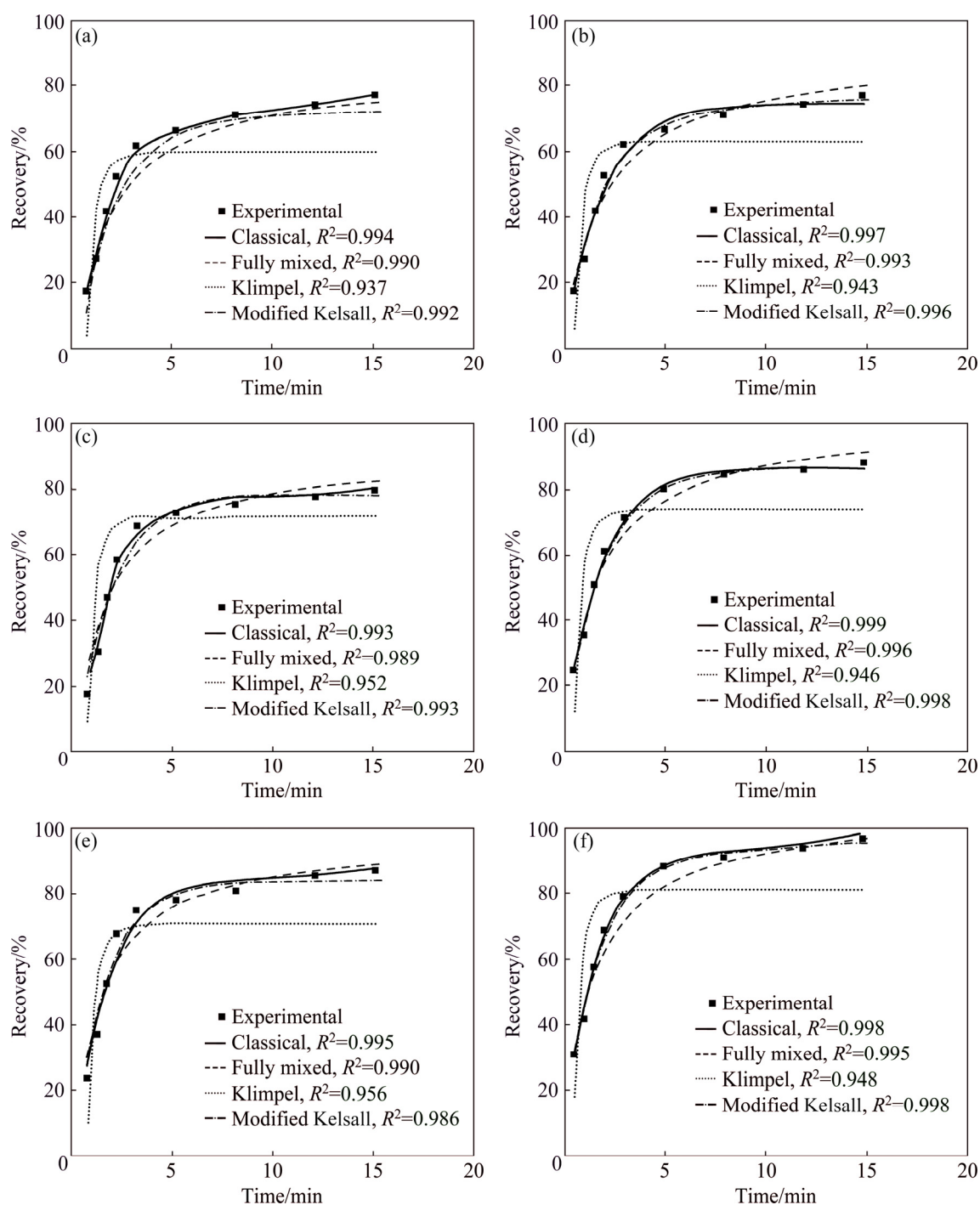


Fig. 2 Comparison of different first-order flotation kinetic models for experimental data before (BS) and after (AS) surface dissolution: (a) IL+Ol-Px, BS; (b) IL+Ol-Px, AS; (c) IL+Tr-Cch, BS; (d) IL+Tr-Cch, AS; (e) IL+Q, BS; (f) IL+Q, AS (pH: 6.3; solid fraction: 30%; collector dosage: 1000 g/t; pine oil dosage: 100 g/t)

Table 3 Estimated kinetic parameters by classical model for ilmenite flotation from binary mixture of minerals

Feed	IL+ Ol-Px				IL+Tr-Cch				IL+Q			
	IL		Ol-Px		IL		Tr-Cch		IL		Q	
	BS	AS	BS	AS	BS	AS	BS	AS	BS	AS	BS	AS
$R_{\infty}/\%$	75.73	80.9	55.2	44.5	76.9	85.2	49.747	35.1	82.1	92.2	33.8	33.95
K/min^{-1}	0.477	0.515	0.512	0.473	0.504	0.537	0.517	0.432	0.583	0.61	0.465	0.462
R^2	0.996	0.997	0.991	0.995	0.995	0.999	0.992	0.995	0.996	0.999	0.996	0.996

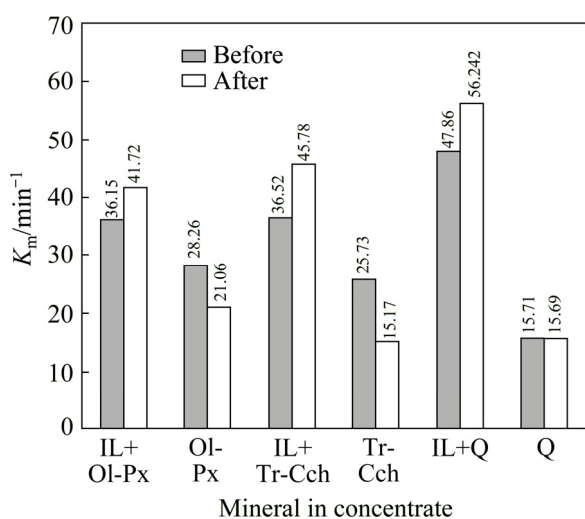


Fig. 3 Comparison of modified rate constant (K_m) for flotation of gangue minerals and ilmenite from binary mixed minerals before and after surface dissolution

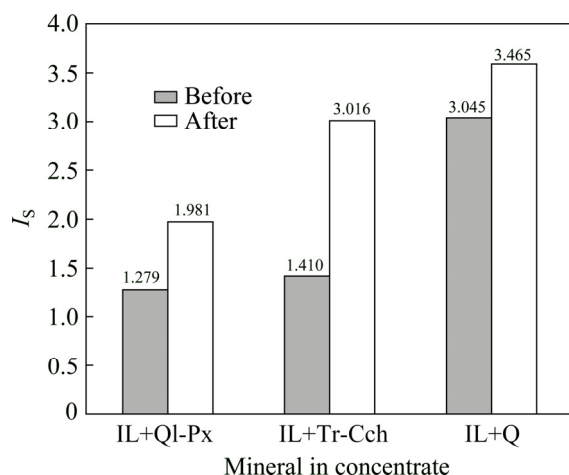


Fig. 4 Comparison of kinetic selectivity index (SI, I_s) for flotation of ilmenite from binary mixed minerals before and after surface dissolution

4.1.4 Optimum time of flotation

In order to produce the eligible concentrate, the flotation of minerals should be completed at a specific time where the separation efficiency is maximized. At this time, the rate of recovery of valuable mineral equal to that of gangue mineral comes into the concentrate. Above this time, the rate of gangue minerals starts to be higher than that of valuable minerals [15,35]. The optimum time of flotation (t_{opt}) can be calculated by the following equation [39]:

$$t_{\text{opt}} = \frac{\ln I_s}{k_v - k_g} \quad (11)$$

where k_v and k_g are the rate constants for valuable and gangue minerals, respectively.

The results of kinetic parameters which were determined by the classic first-order kinetic model are used for calculating the optimum time of flotation (t_{opt}). T_{opt} was calculated for the binary mixtures of minerals before and after surface dissolution. The results shown in Fig. 5 indicate that the surface dissolution increases the t_{opt} for IL+Ol-Px and IL+Tr-Cch mixtures, while it decreases that for IL+Q. It can be found that the more the modified rate constant and ultimate recovery, the more the t_{opt} .

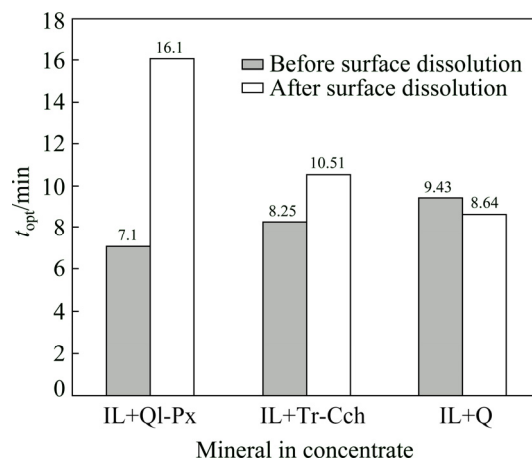


Fig. 5 Comparison of optimum flotation time (t_{opt}) for different binary mixed minerals before and after surface dissolution

4.2 ICP-MS analysis

The liquid phases produced by surface dissolution of purified minerals were analyzed by the ICP-mass method. The results presented in Table 4 show the amounts of Fe^{2+} , Mg^{2+} , Ca^{2+} , Si^{4+} and Ti^{4+} ions releasing from the surface of those minerals. As observed, the dissolution amount of Fe^{2+} , Mg^{2+} and Ca^{2+} ions from the surface of Ol-Px and Tr-Cch phases is much more than that of ilmenite and quartz minerals. By eliminating these metallic ions, the lack of the formation of hydroxyl complexes as the effective groups for interacting with oleate species [40] diminishes the floatability of minerals. Besides, the released ions may form some precipitates on the surface of minerals preventing the collector adsorption and hence their flotation. These events can also affect the kinetic parameters.

Table 4 Content of dissolved ions from ilmenite, Ol-Px, and Tr-Cch after surface dissolution determined by ICP-MS analysis (10^{-6})

Sample	Si	Ca	Fe	Mg	Ti
IL	—	—	140.5	55.63	0.28
Ol-Px	340.5	642.6	1503.4	586.8	—
Tr-Cch	392.7	686.2	437.8	613.6	—
Q	418	69	13	—	—

4.3 Contact angle

The contact angle on the surface of studied minerals was measured as a function of time in the presence of 3.65×10^{-4} mol/L sodium oleate before and after surface dissolution. Figure 6 shows that the contact angle of ilmenite is more than that of accompanying gangue minerals in an extensive period. By rising the time, the measured contact angles for all minerals are decreased with a similar trend. After 3 min the flotation is fast in the first region (Section 3.1), where the contact angles for untreated minerals including ilmenite, Ol-Px, Tr-Cch, and quartz are obtained about 42° , 33° , 30° and 29.7° , respectively. Figure 7 displays that the measured contact angle for pretreated ilmenite is increased in a wide period of time, while it is decreased for all three gangue minerals. The contact angles for pretreated Ol-Px and Tr-Cch are also decreased and come close to that of quartz. This can be due to the removal of Ca^{2+} , Mg^{2+} and Fe^{2+} ions as the surface active sites, interacting with the oleate ions and enhancing the surface hydrophobicity [7,9,40,41]. In other words, when the studied gangue minerals subjected to the surface dissolution, their surface properties are somewhat similar to that of quartz. In the fast flotation region, the contact

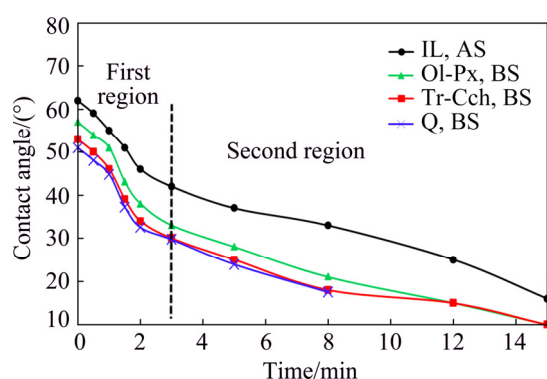


Fig. 6 Measured contact angle for studied minerals as function of time before surface dissolution (pH=6.3; sodium oleate concentration: 3.65×10^{-4} mol/L)

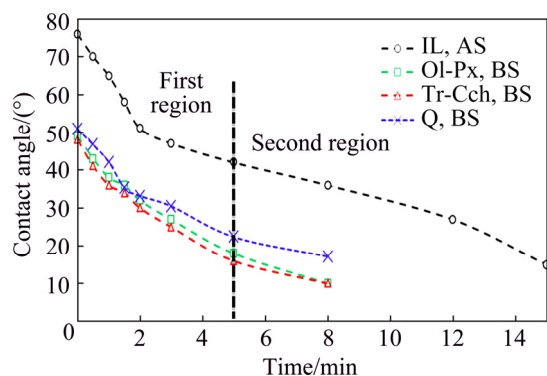


Fig. 7 Measured contact angle for studied minerals as function of time after surface dissolution (pH=6.3; sodium oleate concentration: 3.65×10^{-4} mol/L; dissolution time: 10 min; acid concentration: 7.5 vol.%)

angles for the treated ilmenite, Ol-Px, Tr-Cch, and quartz are achieved almost 42° , 18° , 16° and 22.4° , respectively after 5 min. It is clear that the results of the measured contact angle are in good agreement with the flotation results presented in Fig. 1.

4.4 Scanning electron microscopy (SEM)

Morphology of ilmenite, olivine-pyroxene, and tremolite-clinocllore were investigated by the SEM analysis before and after surface dissolution. The results are shown in Figs. 8(a–f). After surface dissolution, ilmenite somewhat shows a smooth, uniform, and clean surface. In the case of treated gangue minerals, the surface pores and roughness are increased. This can be due to the removal of surface active ions like Fe^{2+} , Ca^{2+} , Mg^{2+} and Al^{3+} from their surfaces through the surface dissolution process. These results are in good accordance with the results of ICP-MS analysis.

4.5 Kinetics of collector adsorption

The kinetics of collector adsorption on ilmenite, olivine-pyroxene, tremolite-clinocllore, and quartz were determined using 3.65×10^{-4} mol/L sodium oleate as a collector in various time intervals at a pH of 6.3 before and after surface dissolution. Two models of the pseudo-first-order and pseudo-second-order were fitted to the experimental data. The results show that the linear form of the pseudo-second-order model which is based on the adsorption capacity of the solid phase (mineral) can well describe the experimental data for all minerals before and after surface dissolution (Fig. 9). This indicates that the chemisorption rate may be the controller step in the procedure [42]. Based on the pseudo-second-order model, the initial adsorption rate is determined by [43]

$$H = K_2 S_e^2 \quad (12)$$

According to the results of kinetic parameters (Table 4), the constant rate of collector adsorption for ilmenite is less than that of all gangue minerals, and the initial adsorption rate of ilmenite is only higher than that of Tr-Cch.

After surface dissolution, the equilibrium capacity of collector adsorption (S_e), rate constant (K_2) and initial adsorption rate (H) for ilmenite are significantly increased while these parameters are decreased for all three gangue minerals. This can be due to the changes in the surface properties of minerals through the surface dissolution. Thus, the surface dissolution process changes the collector adsorption properties of minerals, including adsorption density and adsorption kinetics by changing the number of surface ions and their positions.

It has been shown that the adsorption of reagent on the minerals depends on the surface properties of

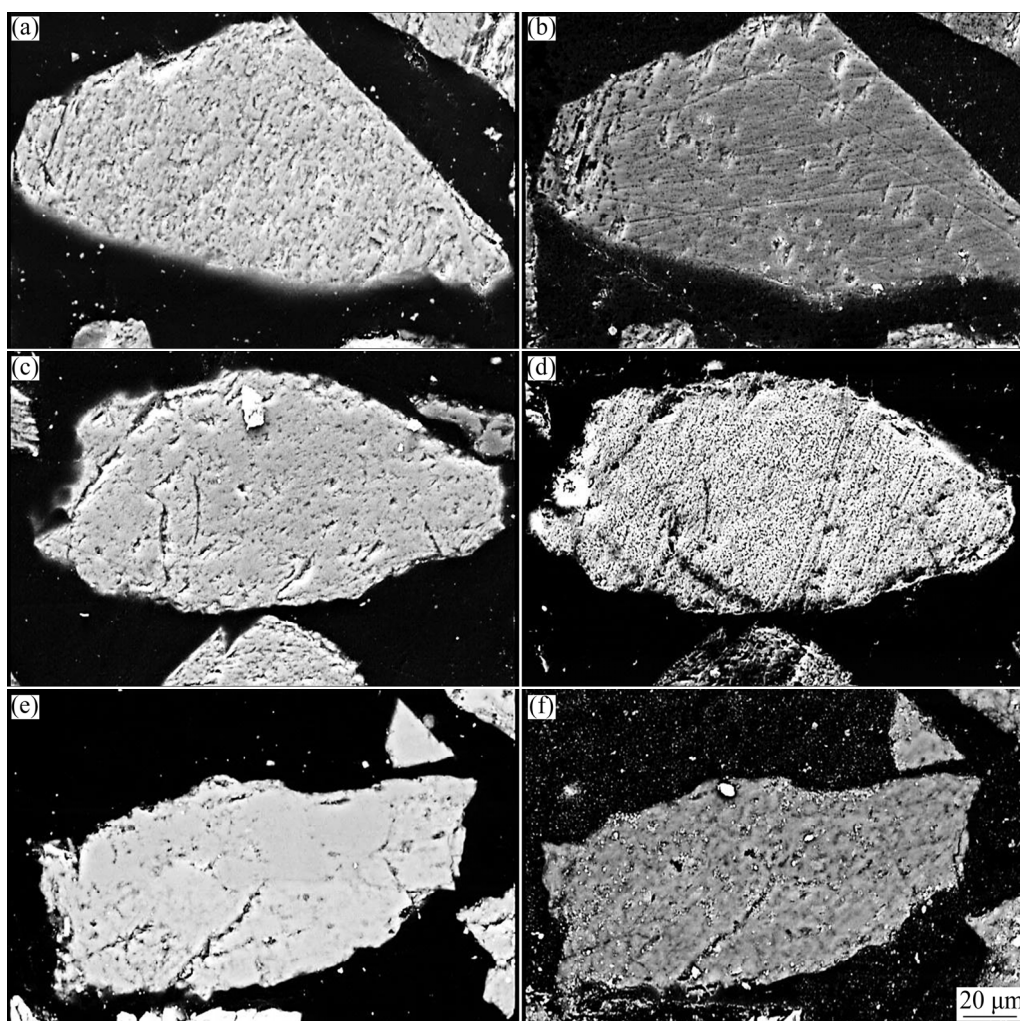


Fig. 8 SEM images of minerals before (a, c, e) and after (b, d, f) acid surface dissolution: (a, b) Ilmenite; (c, d) Olivine-pyroxene; (e, f) Tremolite-clinocllore

minerals, including morphology, mineralogy and surface charge [4,10,44,45] which all of them can be changed after the surface dissolution process.

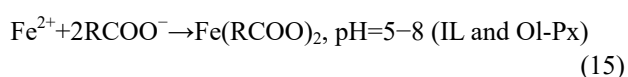
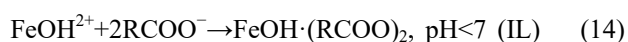
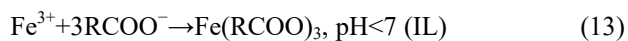
5 Discussion

5.1 Collector adsorption

Collectors adsorb on the surface of minerals through the chemisorption and physisorption mechanisms. For studied minerals including ilmenite, Ol-Px, Tr-Cch and quartz having the iep (isoelectric point) values of 5.4, 3.8, 4.4 and 2.0, respectively [5,46], the adsorption of sodium oleate at a pH of 6.3 takes place dominantly by chemisorption mechanism. The adsorption density of oleate ions on the surface of quartz before and after pretreatment is negligible, which results in the lower flotation recovery of this mineral. This can be due to the lack of reaction of oleate species with Si ions as the only surface cations of quartz. In the case of ilmenite, olivine-pyroxene, and tremolite-clinocllore, the chemisorptions

of oleate species on the surface of minerals are taken place according to Eqs. (13)–(22) [40].

These equations indicate that before surface dissolution Fe^{2+} , Mg^{2+} , Ca^{2+} and their hydroxyl complexes are surface active sites for interacting with oleate species. After surface dissolution, by significant removal of these active sites from the surface of olivine, pyroxene, tremolite and clinocllore, the adsorption density and adsorption kinetics of collector are decreased dramatically for Ol-Px and Tr-Cch samples. In the case of pretreated ilmenite, the increase of collector adsorption density and kinetics can be attributed to the conversion of Fe^{2+} ions to Fe^{3+} ones which have higher tendency for reacting with oleate species [40].



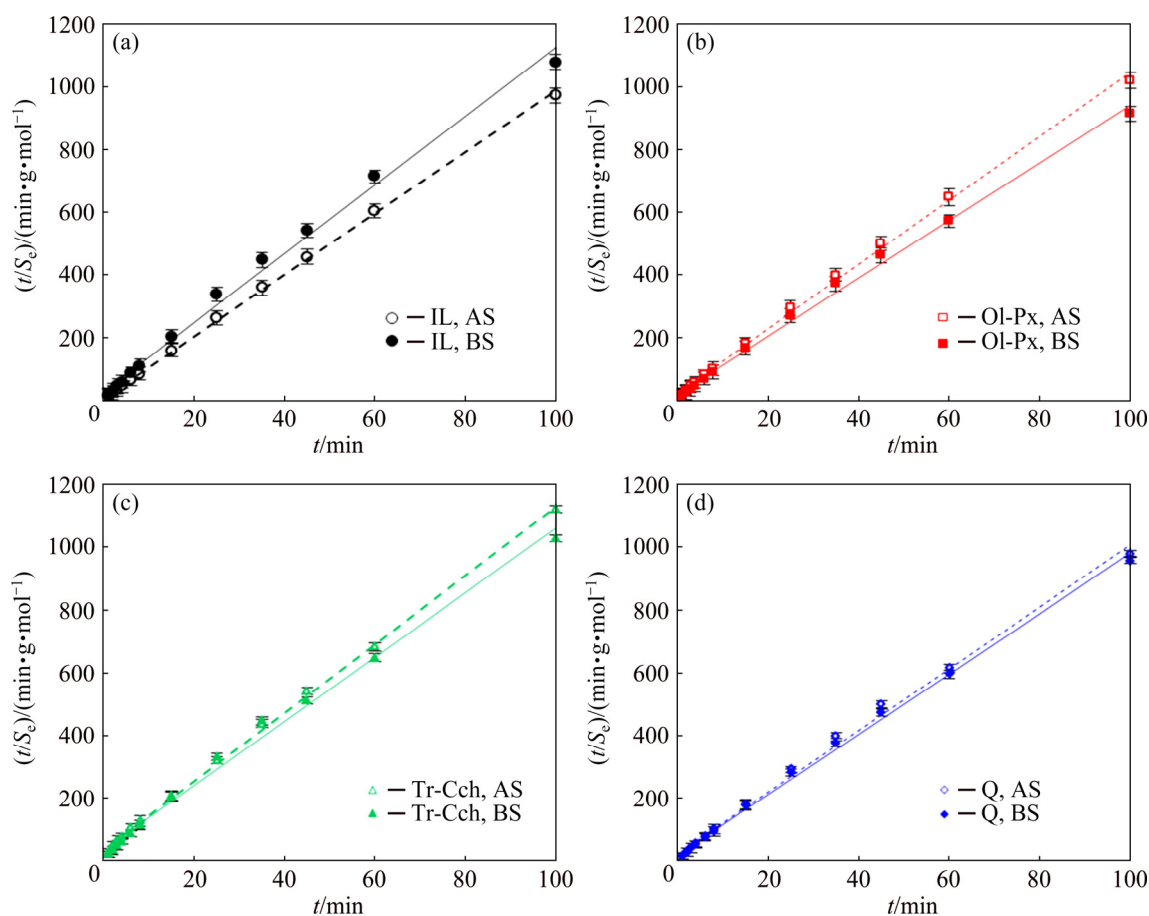
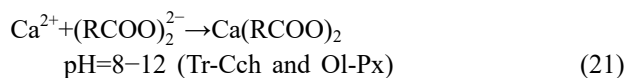
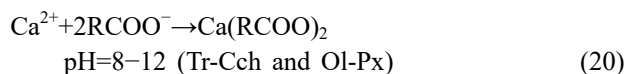
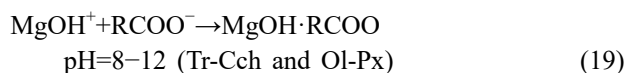
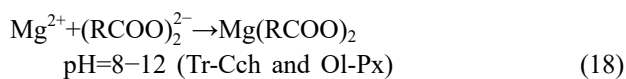
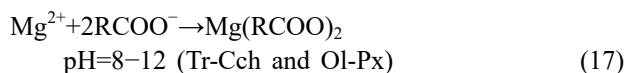
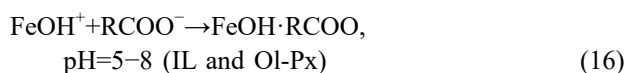


Fig. 9 Pseudo-second-order kinetic model for adsorption of sodium oleate on IL, Ol-Px, Tr-Cch, and quartz at 25 °C before and after surface dissolution: (a) IL; (b) Ol-Px; (c) Tr-Cch; (d) Q

Table 5 Comparison of adsorption kinetics (pseudo-second-order) parameters for IL, Ol-Px, Tr-Cch, and Q at 25 °C before and after surface dissolution

Mineral		$S_e/$ (mol·g ⁻¹)	$K_2/$ (mol·g ⁻¹ ·min ⁻¹)	$H/$ (mol·g ⁻¹ ·min ⁻¹)
IL	Before	0.093	5.272	0.0183
	After	0.105	8.441	0.0943
Ol-Px	Before	0.07	6.332	0.0316
	After	0.06	5.034	0.0183
Tr-Cch	Before	0.041	7.309	0.0123
	After	0.037	6.223	0.0086
Q	Before	0.053	7.774	0.0223
	After	0.051	7.371	0.0195



5.2 Flotation kinetics

The surface dissolution before the flotation changes the surface properties of minerals, controlling the vicinity of the particles and bubbles and changing the collision, attachment and detachment phenomena [3], which in turn changes ultimate recovery and kinetic rate constant of the minerals flotation.

The classical first-order kinetic model, which is named as the first-order with Dirac delta function, is the most applicable kinetic model to portray a flotation process [16,34]. The rate constant takes into account some parameters, including superficial gas velocity, bubble size, collision, and attachment efficiencies, which are shown by Eq. (23) [17,47]:

$$K = \frac{3}{2} \frac{G_{fr} h}{d_b V_{cell}} E_c E_a \quad (23)$$

where G_{fr} is the gas flow rate, h is the height of the flotation cell, d_b is the diameter of the bubble, V_{cell} is the volume of the flotation cell; E_c and E_a are the efficiencies of the bubble-particle collision and attachment, respectively. The bubble-particle collection phenomenon is divided into three events, including collision, attachment, and detachment [48,49].

From flotation kinetics point of view, the particle-bubble collision and attachment are the rate controlling steps in a flotation process [47]. The interfacial properties of a bubble-particle control the phenomena of attachment and detachment. The bubble-particle collision is independent of contact angle, whereas attachment and detachment can be dependent on the contact angle [50–53]. In this regard, the attachment time [54] is defined as the time of a particle-bubble attachment, which is taken into account both hydrodynamic and surface chemistry of flotation. Kinetics of particle-bubble attachment is determined by attachment time [55,56]. KOWALCZUK et al [56] reported that the more hydrophobic the particles, the low attachment time [56].

After surface dissolution, the conversion of Fe^{2+} ions to Fe^{3+} ones on the surface of ilmenite results in the formation of more insoluble ferric iron oleate ($K_{sp}=1 \times 10^{-29.7}$) in comparison with ferrous iron oleate ($K_{sp}=1 \times 10^{-15.5}$) [40]. This means that using sodium oleate as a collector, the hydrophobicity of treated ilmenite is more than that of the original one. This also has been confirmed by the results of contact angle measurements presented in Figs. 6 and 7. The more hydrophobic surface of treated ilmenite causes the decrease of bubble attachment time and the formation of more stable particle-bubble attachment during its climb to the froth phase in the flotation cell. Thus, these events enhance the flotation rate constant for treated ilmenite by increasing the efficiency of bubble-particle attachment (E_a) according to Eq. (23).

In the case of Ol-Px and Tr-Cch phases, by removing some active sites (Fe^{2+} , Mg^{2+} , and Ca^{2+} ions and their hydroxyl species) from the minerals surfaces via surface dissolution, the collector adsorption density is significantly decreased. The decrease of collector adsorption density can also be due to the formation of some precipitate components on the surface of minerals which prevent the interaction between oleate species and minerals active sites. Therefore, the less adsorption density of collector reduces the hydrophobicity (Figs. 6 and 7) of treated minerals including olivine, pyroxene, tremolite, and clinocllore. This affects the stability of bubble-particle attachment negatively and decreases the

flotation rate constant for treated Ol-Px and Tr-Cch phases.

6 Conclusions

(1) Through the surface dissolution pretreatment the significant amount of Fe^{2+} , Mg^{2+} and Ca^{2+} ions dissolved from the surface of gangue minerals such as olivine, pyroxene, tremolite, and clinocllore while the removal of ions from ilmenite surface is negligible.

(2) The removal of active cations from the surface of gangue phases makes great differences between the surface properties of ilmenite and gangue minerals.

(3) After surface modification, the flotation recovery of ilmenite is increased while it is decreased for gangue minerals, especially Ol-Px and Tr-Cch samples.

(4) The adsorption kinetics and initial adsorption rate of the collector is improved for pretreated ilmenite while those are reduced for gangue minerals after pretreatment.

(5) The surface dissolution improves the modified rate constant and kinetic selectivity indices of ilmenite in the presence of all gangue minerals.

(6) In a flotation circuit, the improvement of flotation kinetic parameters through the acid surface dissolution results in the production of high quality concentrate with lower volumes of equipments. This is very important from the economic point of view.

References

- [1] DRZYMALA J. Mineral processing: Foundations of theory and practice of mineralurgy [M]. 1st ed. Wrocław: Ofic Wyd PWR., 2007.
- [2] WILLS B A, FINCH J. Wills' mineral processing technology: An introduction to the practical aspects of ore treatment and mineral recovery [M]. 1st ed. Oxford: Butterworth-Heinemann, 2015.
- [3] VERRELLI D, KOH P, NGUYEN A. Particle– bubble interaction and attachment in flotation [J]. Chemical Engineering Science, 2011, 66: 5910–5921.
- [4] XU Bo, LIU Shuang, LI Hong-qiang, ZHAO Yun-liang, LI Hong-chao, SONG Shao-xian. A novel chemical scheme for flotation of rutile from eclogite tailing [J]. Results in Physics, 2017, 7: 2893–2897.
- [5] RAHIMI S, IRANNAJAD M, MEHDILO A. Effects of sodium carbonate and calcium chloride on calcite depression in cationic flotation of pyrolusite [J]. Transactions of Nonferrous Metals Society of China, 2017, 27: 1831–1840.
- [6] FAN Xian-feng, WATERS K, ROWSON N, PARKER D. Modification of ilmenite surface chemistry for enhancing surfactants adsorption and bubble attachment [J]. Journal of Colloid and Interface Science, 2009, 329: 167–172.
- [7] ZHU Yang-ge, ZHANG Guo-fan, FENG Qi-ming, YAN Dai-cui, WANG Wei-qing. Effect of surface dissolution on flotation separation of fine ilmenite from titanite [J]. Transactions of Nonferrous Metals Society of China, 2011, 21: 1149–1154.
- [8] ZHAI Ji-hua, CHEN Pan, WANG Hong-bin, HU Yue-hua, SUN Wei. Floatability improvement of ilmenite using attrition-scrubbing as a pretreatment method [J]. Minerals, 2017, 7: 1–13.

- [9] SALMANI NURI O, IRANNAJAD M, MEHDILO A. Microwave irradiation consequences on chemical reagent consumption in ilmenite flotation [J]. *Journal of Microwave Power and Electromagnetic Energy*, 2017, 51: 93–105.
- [10] YU Li, YING Lei, ZHANG Li-bo, PENG Jin-hui, LI Chang-long. Microwave drying characteristics and kinetics of ilmenite [J]. *Transactions of Nonferrous Metals Society of China*, 2011, 21: 202–207.
- [11] FAN Xian-feng, ROWSON N. Fundamental investigation of microwave pretreatment on the flotation of massive ilmenite ores [J]. *Asia-Pacific Journal of Chemical Engineering*, 2000, 8: 167–182.
- [12] SONG Quan-yuan, TSAI S. Flotation of ilmenite using benzyl arsonic acid and acidified sodium silicate [J]. *International Journal of Mineral Processing*, 1989, 26: 111–121.
- [13] SEMSARI P P, IRANNAJAD M, MEHDILO A. Modification of ilmenite surface properties by superficial dissolution method [J]. *Minerals Engineering*, 2016, 92: 160–167.
- [14] SEMSARI P P, IRANNAJAD M, MEHDILO A. Effect of acid surface dissolution pretreatment on the selective flotation of ilmenite from olivine and pyroxene [J]. *International Journal of Mineral Processing*, 2017, 167: 49–60.
- [15] AGAR G E, CHIA J, REQUIS C L. Flotation rate measurements to optimize an operating circuit [J]. *Minerals Engineering*, 1998, 11: 347–360.
- [16] LYNCH A, JOHNSON N, MANLAPIG E, THORNE C. Mineral and coal flotation circuits: Their simulation and control [M]. Vol.65. Amsterdam: Elsevier, 1981.
- [17] RALSTON J. The influence of particle size and contact angle in flotation (Developments in mineral processing) [M]. Elsevier; 1992, 203–224.
- [18] UÇURUM M. Influences of Jameson flotation operation variables on the kinetics and recovery of unburned carbon [J]. *Powder Technology*, 2009, 191: 240–246.
- [19] AGAR G. Optimizing the design of flotation circuits [J]. *Canadian Mining and Metallurgical Bulletin*, 1980, 73: 173–181.
- [20] ROWN D J, SMITH H G. The flotation of coal as a rate process [J]. *Transactions of the American Institute of Mining, Metallurgical Engineers*, 1954, 113: 1001.
- [21] KLIMPEL R. Selection of chemical reagents for flotation [M]. New York: Mineral Processing Plant Design, 1980, 2: 907–934.
- [22] VANANGAMUDI M. Modelling and kinetic studies on coal flotation and coal-oil agglomeration processes [D]. Dhanbad, India: Indian School of Mines, 1983.
- [23] OLIVEIRA J F, SARAIVA S M, PIMENTA J S, OLIVEIRA A P A. Kinetics of pyrochlore flotation from Araxa mineral deposits [J]. *Minerals Engineering*, 2001, 14: 99–105.
- [24] SOKOLOVIĆ J M, STANOJLOVIĆ R, MARKOVIĆ Z. The effects of pretreatment on the flotation kinetics of waste coal [J]. *International Journal of Coal Preparation and Utilization*, 2012, 32: 130–142.
- [25] STANOJLOVIĆ R, SOKOLOVIĆ J. A study of the optimal model of the flotation kinetics of copper slag from copper mine Bor [J]. *Archives of Mining Sciences*, 2014, 59: 821–834.
- [26] AZIZI A, HASSANZADEH A, FADAEI B. Investigating the first-order flotation kinetics models for Sarcheshmeh copper sulfide ore [J]. *International Journal of Mining Science and Technology*, 2015, 25: 849–854.
- [27] WOLFARM S. The Mathematica book [M]. Cambridge: Wolfram Media Inc, Cambridge Univ. Press, 2003.
- [28] IRANNAJAD M, MEHDILO A. Concentration of Iranian titanium ore by physical methods [C]//International Gravity Concentration Symposium. Tehran, Iran: Scientific Information Database, 2004.
- [29] DEER W A, ANDREW H R, ZUSSMAN J. An introduction to the rock-forming minerals [J]. *Mineralogical Magazine*, 1992: 56(385): 617–619.
- [30] MEHDILO A, IRANNAJAD M, REZAI B. Effect of oxidation roasting on ilmenite flotation [J]. *Physicochemical Problems of Mineral Processing*, 2014, 50: 493–505.
- [31] MEHDILO A, IRANNAJAD M. Comparison of microwave irradiation and oxidation roasting as pretreatment methods for modification of ilmenite physicochemical properties [J]. *Journal of Industrial and Engineering Chemistry*, 2016, 33: 59–72.
- [32] MEHDILO A, IRANNAJAD M, REZAI B. Effect of crystal chemistry and surface properties on ilmenite flotation behavior [J]. *International Journal of Mineral Processing*, 2015, 137: 71–81.
- [33] MEHDILO A, IRANNAJAD M, REZAI B. Effect of chemical composition and crystal chemistry on the zeta potential of ilmenite [J]. *Colloids and Surfaces A: Physicochemical and Engineering Aspects*, 2013, 428: 111–119.
- [34] BU Xiang-ning, XIE Guang-yuan, PENG Yao-li, GE Lin-han, NI Chao. Kinetics of flotation. order of process, rate constant distribution and ultimate recovery [J]. *Physicochemical Problems of Mineral Processing*, 2017, 53: 342–365.
- [35] AGAR G E. Simulation in mineral processing. in mineral processing design [M]. Dordrecht: Springer, 1987: 268–287.
- [36] UÇURUM M, BAYAT O. Effects of operating variables on modified flotation parameters in the mineral separation [J]. *Separation and Purification Technology*, 2007, 55: 173–181.
- [37] SRIPRIYA R, RAO P, CHOUDHURY R B. Optimisation of operating variables of fine coal flotation using a combination of modified flotation parameters and statistical techniques [J]. *International Journal of Mineral Processing*, 2003, 68: 109–127.
- [38] AZIZI A. A study on the modified flotation parameters and selectivity index in copper flotation [J]. *Particulate Science and Technology*, 2017, 35: 38–44.
- [39] CILEK E C. Estimation of flotation kinetic parameters by considering interactions of the operating variables [J]. *Minerals Engineering*, 2004, 17: 81–85.
- [40] ZHONG Kang-nien, LIN Cui. Influence of Fe^{2+} ions of ilmenite on its flotability [J]. *International Journal of Mineral Processing*, 1987, 20: 253–265.
- [41] SALMANI NURI O, MEHDILO A, IRANNAJAD M. Influence of microwave irradiation on ilmenite surface properties [J]. *Applied Surface Science*, 2014, 311: 27–32.
- [42] WANG Bo, PENG Yong-jun. The effect of saline water on mineral flotation—A critical review [J]. *Minerals Engineering*, 2014, 66: 13–24.
- [43] XING Yao-wen, GUI Xia-hui, PAN Lei, PINCHASIK Bat-el, CAO Yi-jun, LIU Jiong-tian, BUTT Hans-jürgen. Recent experimental advances for understanding bubble-particle attachment in flotation [J]. *Advances in Colloid and Interface Science*, 2017, 246: 105–132.
- [44] CHEN Hai-han, GRASSIAN V H. Iron dissolution of dust source materials during simulated acidic processing: The effect of sulfuric, acetic, and oxalic acids [J]. *Environmental Science & Technology*, 2013, 47: 10312–10321.
- [45] IRANNAJAD M, SALMANI N O, MEHDILO A. Surface dissolution-assisted mineral flotation: A review [J]. *Journal of Environmental Chemical Engineering*, 2019, 7: 103050.
- [46] IRANNAJAD M, SALMANI N O, MEHDILO A. Influence of microwave irradiation on ilmenite flotation behavior in the presence of different gangue minerals [J]. *Separation and Purification Technology*, 2014, 132: 401–412.
- [47] JAMESON G J, NAM S, YOUNG M. Physical factors affecting recovery rates in flotation [J]. *Minerals Science and Engineering*, 1977, 9: 103–118.
- [48] NGUYEN A V, SCHULTZE H J. Colloidal science of flotation [M]. 1st ed. New York: Marcel Dekker Inc, 2004.

- [49] ALBIJANIC B, OZDEMIR O H, NGUYEN A, BRADSHAW D. A review of induction and attachment times of wetting thin films between air bubbles and particles and its relevance in the separation of particles by flotation [J]. *Advances in Colloid and Interface Science*, 2010, 159: 1–21.
- [50] CHAU T T, BRUCKARD W J, KOH P T L, NGUYEN A V. A review of factors that affect contact angle and implications for flotation practice [J]. *Advances in Colloid and Interface Science*, 2009, 150: 106–15.
- [51] KOUACHI S, VAZIRI H B, HASSANZADEH A, ÇELİK S M, BOUHENGUEL M. Effect of negative inertial forces on bubble-particle collision via implementation of Schulze collision efficiency in general flotation rate constant equation [J]. *Colloids and Surfaces A: Physicochemical and Engineering Aspects*, 2017, 517: 72–83.
- [52] SCHULZE H J. Hydrodynamics of bubble-mineral particle collisions [J]. *Mineral Processing and Extractive Metallurgy Review*, 1989, 5: 43–76.
- [53] DAI Zong-fu, FORNASIERO D, RALSTON J. Particle-bubble collision models—A review [J]. *Advances in Colloid and Interface Science*, 2000, 85: 231–256.
- [54] SVEN N. Effect of contact time between mineral and air bubbles on flotation [J]. *Kolloid-Z*, 1934, 69(2): 230–232.
- [55] KRASOWSKA M, MALYSA K. Wetting films in attachment of the colliding bubble [J]. *Advances in Colloid and Interface Science*, 2007, 134: 138–150.
- [56] KOWALCZUK P, ZAWALA J. A relationship between time of three-phase contact formation and flotation kinetics of naturally hydrophobic solids [J]. *Colloids and Surfaces A: Physicochemical and Engineering Aspects*, 2016, 506: 371–377.

表面溶解对从不同脉石矿物中 浮选分离钛铁矿的动力学参数的影响

Omid SALMANI NURI¹, Mehdi IRANNAJAD¹, Akbar MEHDILO^{1,2}

1. Department of Mining and Metallurgical Engineering, Amirkabir University of Technology, Tehran, Iran;

2. Department of Engineering, University of Mohaghegh Ardabili, Ardabili, Iran

摘 要: 研究表面酸溶解对钛铁矿(IL)及其常见伴生脉石矿物(包括橄榄石-辉石(Ol-Px)、透闪石-斜绿泥石(Tr-Cch)和石英)浮选动力学的影响。结果表明,通过表面溶解,钛铁矿的吸附速率常数从 5.272 增大到 8.441 mol/(g·min),而 Ol-Px、Tr-Cch 和石英的吸附速率常数分别从 6.332、7.309 和 7.774 mol/(g·min)减小为 5.034、6.223 和 7.371 mol/(g·min)。二元混合矿物的浮选实验结果表明,经表面溶解后,从 Ol-Px、Tr-Cch 和石英中浮选钛铁矿的修正速率常数分别分别 36.15、36.52 和 47.86 min⁻¹ 增大到 41.72、45.78 和 56.24 min⁻¹,导致从脉石矿物中分离预处理过的钛铁矿过程的动力学选择性指数(SI)增大。ICP-MS 分析证实,脉石矿物动力学参数的降低可能是由于其表面 Fe²⁺、Ca²⁺和 Mg²⁺的去除,导致矿物表面缺乏足够的活性位点与捕集剂组分发生作用。接触角测量结果证实,表面溶解可防止矿物表面形成稳定的疏水层,从而可在矿物和气泡之间发生稳定的附着。一般来说,钛铁矿浮选动力学参数的提高与伴生脉石矿物中的铁含量呈负相关关系。

关键词: 表面溶解; 浮选; 动力学参数; 修正速率常数; 选择性指数; 捕集剂吸附

(Edited by Xiang-qun LI)